Feedforward-feedback Controller using General Regression Neural Network (GRNN) for Laboratory HVAC System: Part II—Temperature Control—Cooling

Osman Ahmed, Ph.D., P.E.
Member ASHRAE

John W. Mitchell, Ph.D., P.E.
Fellow ASHRAE

Sanford A. Klein, Ph.D.
Fellow ASHRAE

ABSTRACT

This is the second part of a three-part paper on feedforward controllers for laboratory HVAC control systems. The development of a controller for temperature during the cooling sequence is studied. Internal heat generation in the laboratory space is the primary disturbing force that activates this sequence. Additional cooling is provided to offset increased load by supplying additional air into the space. The supply flow rate is increased by first opening the general exhaust damper to increase the total laboratory exhaust flow rate. The laboratory pressure constraint is met first, and this is followed by the control on temperature. The combined feedforward-feedback approach is found to outperform the conventional feedback controller.

INTRODUCTION

In Part I (Ahmed et al. 1998a) of this paper on feedforward controllers, the unique aspects of a laboratory HVAC system are highlighted and the opportunity of achieving energy savings with the variable-air-volume (VAV) system is presented. A combined feedforward and feedback control approach is proposed as an alternative solution to the present approach of feedback control, i.e., proportional-integral-derivative (PID), for a laboratory HVAC control system. The combined approach uses a general regression neural network (GRNN) to identify the parameter of the component characteristics and control. The combined approach shows good results in terms of providing stable and accurate pressure control over a wide operating range and with different damper characteristics. This paper explores the applicability of the combined approach for temperature control during cooling sequences commonly found in a laboratory.

The cooling sequence is described first. The implementation of a combined approach for cooling is discussed next. The details of the simulation of the temperature control sequence are then presented, followed by a comparison of the results and the conclusions.

SEQUENCE FOR TEMPERATURE CONTROL—COOLING

Internal heat generation is the primary disturbing force that activates a need for cooling. The generation rate can increase manyfold rapidly due to activities and equipment in a laboratory. When the internal generation suddenly increases, the room temperature rises rapidly. The only cooling source available is the supply airstream, which is usually at 55°F (12.77°C), and, thus, the supply flow must be increased. Increasing the lab exhaust flow will upset the lab space pressure. In order to circumvent this problem, another source of the exhaust (i.e., general exhaust) is opened to allow an increased supply flow. By artificially increasing the total lab exhaust, both room temperature and the pressure set points are maintained. Figure 1 shows the cooling sequence schematically.

IMPLEMENTATION OF A COMBINED CONTROLLER FOR COOLING

The implementation scheme for the combined controller is similar to what is discussed for the pressure control sequence in Part I (Ahmed et al. 1998a). Two separate combined feedforward and feedback controllers are used for cooling. One is for the supply flow loop and the other one is for the general exhaust flow. Each controller uses the GRNN to identify the damper characteristics and then produce the

Osman Ahmed is a senior principal engineer at Landis and Staefa, Inc., Buffalo Grove, Ill. John W. Mitchell and Sanford A. Klein are professors at the Solar Energy Laboratory at the University of Wisconsin, Madison.
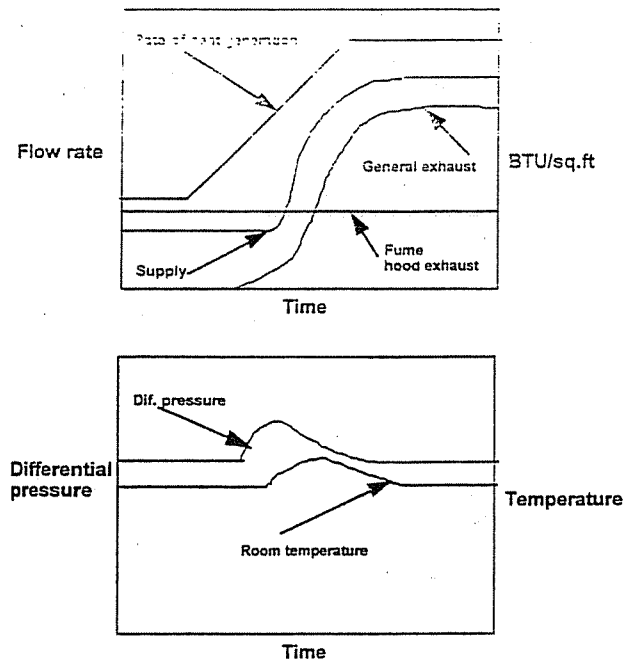
Figure 1 *Temperature control—cooling sequence.*

feedforward block output for the given set points, which are determined based on the method described in the last section. It is expected that by using individual combined controllers for supply and general exhaust flow loops, the implementation process will be much simpler since the GRNN will need to identify and update the individual damper characteristics using only a small set of data. The implementation scheme is shown in Figure 2.
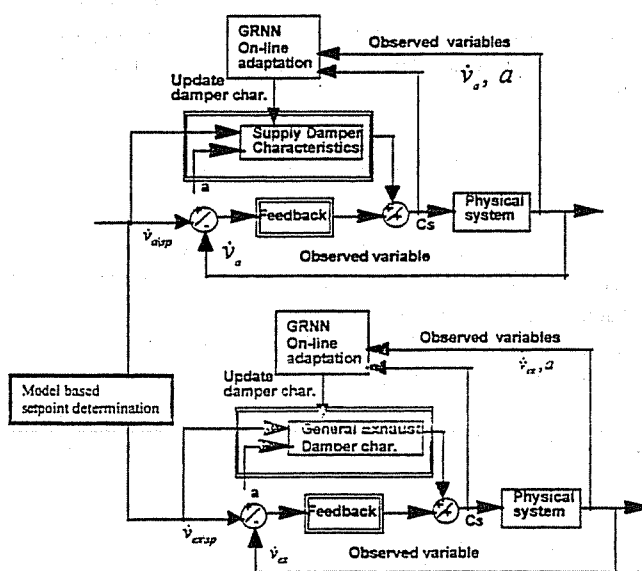

Figure 2 *Implementation of combined controller for temperature control—cooling.*

Temperature Control: Cooling Sequence

Based on the observed results obtained from the pressure control study, the following changes were made for temperature control sequence.

1. Only three damper curves were considered: linear; nonlinear ($W_f = 0.5$) with an authority of 0.01, and a linear damper with an authority of 0.01. Along with the linear damper. the two extreme damper characteristics (shown in Figure 6. Part I) were judged to be sufficient enough to test the various control loops.

2. Only proportional-integral (PI) and combined feedforward and feedback (FFPI) control loops are considered. The response of the feedforward (FF) control loop was very predictable in terms of having a slight offset from set points and still providing stability.

The change in the internal load is the main cause or disturbing function for cooling. Figure 3 shows two internal load curves used in the simulation. In the first case, the generation is increased fivefold from its initial value of 85.50 Btu/min to 427.50 Btu/min (90 kJ/min to 450 kJ/min); in the second case, the internal load is decreased from a higher value to a lower value. The fivefold change in internal heat generation rate within seconds is not uncommon in lab environments (Newman 1989).

The flow set points of the general exhaust and, consequently, of the supply are determined using steady-state energy, mass, and infiltration equations. The energy equation contains a room load term that is calculated based on the room air temperature and the supply flow rate at a preceding time interval. The details of supply flow rate determination and the prediction of room load are discussed in the next section.

Once the set points are known, the FFPI control loop employs the combination of feedforward and feedback approaches to reach the set point. In contrast, the PI control
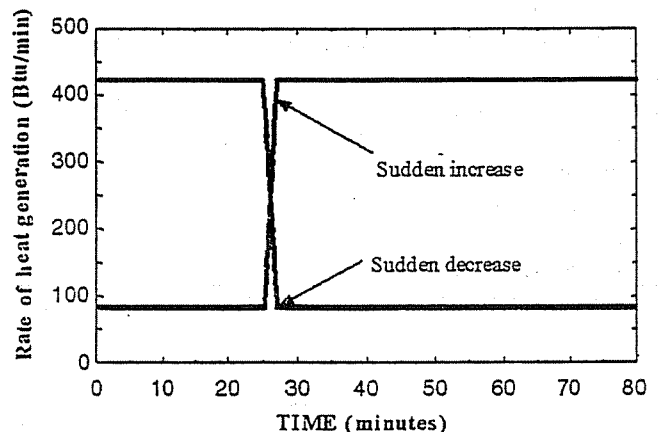

Figure 3 *Disturbance in the rate of heat generation for cooling sequence.*

loop uses only feedback. The success of both methods depends largely upon the accuracy of the load prediction. Since the predicted load is calculated based on previous samples of room temperature and flows, which then influence the flow set points for the next sample, any significant deviation from the room conditions will propagate rapidly via the input for predicted load. The schematics of both FFPI and PI control loops as used in simulation are shown in Figure 4.

Due to the presence of two coupled control loops, the operation of the control sequence is complicated compared to the pressure control that uses a single loop. The tuning of two PI control loops also becomes complicated. In the industry, another PID is employed to determine the set point; this further complicates the tuning process. To avoid such complications, it was decided to use the model-based set points for the PI loops, as well for the simulation. The PI and FFPI are then compared on the same basis of controlling the dampers.

For the temperature control loops, the simulation sample time is selected to be ten seconds. This is much longer than the one-tenth of a second considered for the pressure control loops since the room thermal time constant is found to be about four minutes instead of one-third of a second as for the flow loop. The room temperature response under an open loop test when the supply flow rate at 55°F (12.77°C) is increased to maximum is shown in Figure 5. The room thermal time constant is determined from the open loop response in a similar way as described in Part I (Ahmed et al. 1998a) for determining supply flow time constant.

A sample time of ten seconds means that 24 samples are made within one time constant, which should be more than adequate for a digital controller. Any smaller sample time poses the problem of storing a massive amount of data necessary for simulation considering the entire simulation period for temperature control, which extends to more than an hour.
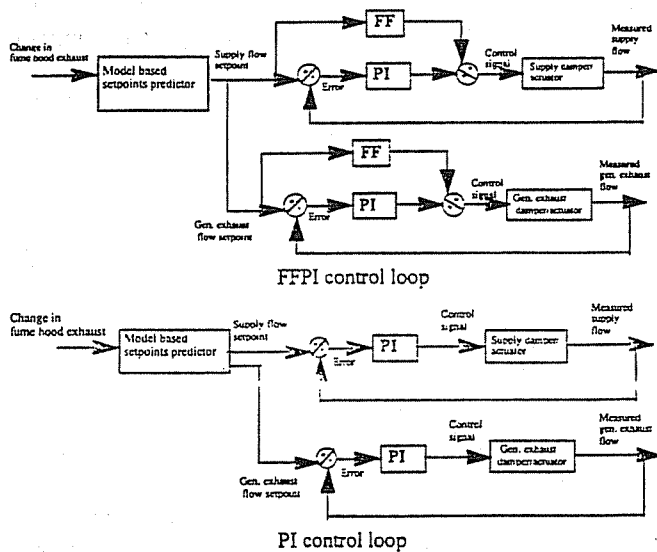
A long simulation period is necessary to ensure that the steady state is reached after a disturbance is introduced.

However, choosing a large sample time posed a problem with the pressure control loop. The time derivative of pressure became so large for a large sample time that the simulation failed to converge. In order to resolve such problems, the time derivative of pressure was ignored and the transient energy and mass balance equations (i.e., Equations 7 and 11) are rewritten as

$$V\left[-\frac{P}{T^2}\frac{dT}{dt}\right] = \frac{P_s \dot{v}_s}{RT_s} + \frac{P_{ad}\dot{v}_{ad}}{RT_{ad}} - \frac{P\dot{v}_e}{RT} \tag{1}$$

$$\frac{P_s \dot{v}_s}{R}c_p + \frac{P_{ad}\dot{v}_{ad}}{R}c_p - \frac{P\dot{v}_e}{R}c_p + \dot{q}_{gen} + \dot{q}_{tr} = 0 \tag{2}$$

The assumption of ignoring the pressure derivative term is justified since, in reality, the fast pressure control loops will always achieve the set point even before the next room temperature is sampled because the room thermal loop is so slow. To ensure that the pressure control loops will act much faster than the room thermal response, the ratio between the sample time and time constant in the exponential term, b in the solution for damper command signal (Equations 14 and 15 of Part I) is chosen to be 3.30. As a result, the damper command signal in the next sample time will be almost equal to the damper command set point, r_{sp}. The expression for damper command signal is repeated below.

$$r_{ac} = br_{ac,(t-t_o)} + (1-b)r_{sp,(t-t_o)} \tag{3}$$

where

$$b = e^{-\left(\frac{S_t}{\tau_{act}}\right)} \tag{4}$$

MODEL-BASED SET POINT DETERMINATION

In the cooling sequence, both supply and general exhaust flow set points need to be determined. A common approach in a feedback controller is to use another PID algorithm that acts
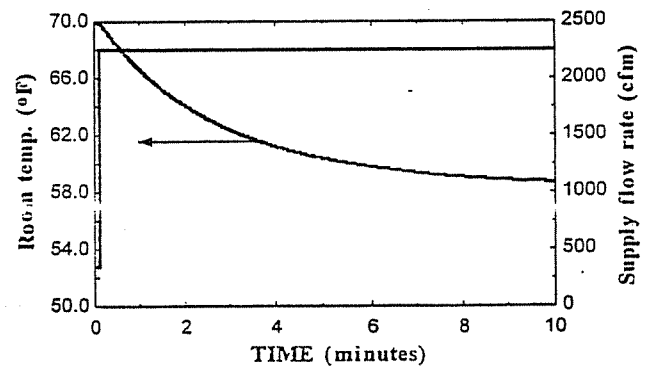
FFPI control loop

PI control loop

Figure 4 *Schematics of control loops for temperature control—cooling sequence.*

Figure 5 *Open loop response of room temperature due to cooling.*

upon the error between the room temperature set point and the actual value. The PID output is the general exhaust flow set point. The supply flow set point is then calculated assuming a fixed differential with respect to the general exhaust flow set point. Addition of another PID loop further complicates the tuning process. With reference to Figure 4, if a PID loop is used instead of a model-based predictor, a total of seven tuning parameters need to be evaluated for the two PI and the one PID coupled loops. The performance of coupled loops also suffers when the operating condition shifts from the tuned condition, a common feature of a laboratory control system. On the other hand, a model-based setpoint predictor will require less tuning and performance will not be dependent on the operating conditions.

The flow set points for general exhaust and, consequently, for supply flow are determined using steady-state energy, mass, and infiltration equations. The steady-state mass and infiltration equations are described for pressure control sequence in Part I and repeated below.

The conservation of mass of air in the laboratory is given by

$$\frac{dm}{dt} = \dot{m}_s + \dot{m}_{ad} - \dot{m}_e. \tag{5}$$

Using the ideal gas law for the density and expressing mass flow in terms of pressure, temperature, and volume flow rate, Equation 1 becomes

$$\frac{d(PV/RT)}{dt} = \frac{P_s\dot{v}_s}{RT_s} + \frac{P_{ad}\dot{v}_{ad}}{RT_{ad}} - \frac{P\dot{v}_e}{RT}. \tag{6}$$

Differentiating the first term by parts and canceling the gas constant, R, on both sides results in

$$\frac{V}{R}\left[\frac{1}{T}\frac{dP}{dt} - \frac{P}{T^2}\frac{dT}{dt}\right] = \frac{P_s\dot{v}_s}{RT_s} + \frac{P_{ad}\dot{v}_{ad}}{RT_{ad}} - \frac{P\dot{v}_e}{RT}. \tag{7}$$

The steady-state mass balance equation then becomes

$$\frac{P_s\dot{v}_s}{RT_s} + \frac{P_{ad}\dot{v}_{ad}}{RT_{ad}} - \frac{P\dot{v}_e}{RT} = 0. \tag{8}$$

The conservation of energy equation includes the energy carried in and out by flows and heat flows.

$$\frac{dU}{dt} = \sum h_i\dot{m}_i - h_e\dot{m}_e + \dot{q}_{gen} + \dot{q}_{tr} \tag{9}$$

where i denotes all inflow, e denotes all outflow, $\dot{q}_{gen}$ is the internal energy generation, and $\dot{q}_{tr}$ is the heat transfer through the envelope.

Equation 9 can be further expanded in terms of mass and specific internal energy as

$$m\frac{du}{dt} + u\frac{dm}{dt} = \sum h_i\dot{m}_i - h_e\dot{m}_e + \dot{q}_{gen} + \dot{q}_{tr}. \tag{10}$$

Taking derivatives of the left-hand side of Equation assuming a constant room volume V, introducing the ideal gas equation for internal energy $u = c_vT$, and expressing mass flow rate in terms of pressure, temperature, volume flow rate, and enthalpy $h = c_pT$, the following equation is obtained.

$$\frac{PV}{RT}c_v\frac{dT}{dt} + \frac{Tc_vV}{RT}\frac{dP}{dt} - c_vT\frac{PV}{RT^2}\frac{dT}{dt} =$$
$$\frac{P_s\dot{v}_s}{RT_s}c_p + \frac{P_{ad}\dot{v}_{ad}}{RT_{ad}}c_p - \frac{P\dot{v}_e}{RT}c_p + \dot{q}_{gen} + \dot{q}_{tr} \tag{11}$$

The steady-state form of the above energy equation then becomes

$$\frac{P_s\dot{v}_s}{RT_s}c_p + \frac{P_{ad}\dot{v}_{ad}}{RT_{ad}}c_p - \frac{P\dot{v}_e}{RT}c_p + \dot{q}_{load} = 0 \tag{12}$$

where

$$\dot{q}_{load} = \dot{q}_{gen} + \dot{q}_{tr}.$$

The infiltration relation is

$$\dot{v}_{ad,sp} = K_l(\Delta P_{sp})^n. \tag{13}$$

The laboratory pressure differential, ΔP_{sp}, is defined as a differential:

$$\Delta P_{sp} = P_{ref,sp} - P_{sp}. \tag{14}$$

Besides room thermal load (sum of terms $\dot{q}_{gen}$ and $\dot{q}_{tr}$ in Equation 11), there are nine variables in Equations 8 and 12 comprising the temperature, flow rate, and pressure of three airstreams: supply, infiltration, and lab exhaust. The room set points for temperature and pressure infiltration are known. The volumetric flow rate of infiltrating air at the set point, $\dot{v}_{ad|sp}$, is also known from Equations 13 and 14. Similarly, the supply air pressure, $P_{s|sp}$, room pressure, $P|_{sp}$, and temperature, $T|_{sp}$, set points are given from design data. There are three unknowns: lab supply airflow rate, $\dot{v}_{s|sp}$; total lab exhaust set point, $\dot{v}_{e|sp}$; and supply air discharge temperature set point, $T_{s|sp}$. The total lab exhaust is a sum of general exhaust and exhaust from fume hoods and is given by

$$\dot{v}_{e|sp} = \dot{v}_{fh|sp} + \dot{v}_{ex|sp}. \tag{15}$$

In a VAV lab, the fume hood exhaust set point is a known quantity for each position of the fume hood sash. Hence, by determining the set point for total lab exhaust, the general exhaust set point will be known.

In order to solve for either supply air discharge temperature or general exhaust set point, Equations 8, 12, 13, 14, and 15 must be solved simultaneously. When the supply air discharge temperature set point is to be determined, then the general exhaust is usually a known quantity and vice versa. The need for determining the desired supply air discharge

4

temperature arises in the heating sequence that is discussed in a companion paper, Ahmed et al. 1998).

The general exhaust is needed when fume hoods are closed and the internal heat generation rate is increased due to process or equipment operation. The room, under such situations, needs more cooling. However, providing additional cooling by just increasing the volumetric flow rate of 55°F (12.77°C) supply air will upset the room pressure equilibrium. As a result, the general exhaust damper needs to be opened to allow more supply air to satisfy the added cooling need. The controller has to determine and control the general exhaust flow rate and supply airflow rate in order to maintain the room pressure and temperature set points. The supply air temperature at 55°F (12.77°C) remains fixed.

In Equation 12, the space thermal load, $\dot{q}_{load}$, needs to be determined in order to obtain the set points. The total cooling load can be determined by using Equation 16, which relates the load to the total lab exhaust flow rate, room temperature, and the supply flow rate at the preceding sample time, $t-1$. In developing the control relations, the air density is assumed to be constant and identical for supply, exhaust, and infiltration air.

$$\dot{q}_{load|ss} = \dot{v}_{e,(t-1)}\rho c_p T_{(t-1)} - \dot{v}_{s,(t-1)}\rho c_p T_s - \dot{v}_{ad|sp}\rho c_p T_{ad}$$
(16)

The total lab exhaust is expressed as a sum of general exhaust and fume hood exhaust flows,

$$\dot{v}_e = \dot{v}_{s,(t-1)} + \dot{v}_{ad|sp}.$$
(17)

In both Equations 16 and 17, it has been found best to use the infiltration flow rate set point, $\dot{v}_{ad|sp}$, instead of the actual infiltration flow rate, $\dot{v}_{ad}$, to avoid an oscillation in the room load prediction. The transients in ΔP introduce oscillations in both the infiltration flow rate, $\dot{v}_{ad}$, and room temperature, T. As a result, the calculated room cooling load will oscillate.

The room temperature, T, can be measured directly by placing the temperature sensor in the room exhaust duct instead of following the usual practice of using a wall room thermostat. In most labs, the exhaust from the fume hoods and the lab are ducted together and the common intersection between the two exhaust streams provides a good location for a duct temperature sensor. Due to the high ventilation requirement, the air in a laboratory space is well mixed and, therefore, exhaust air temperature is a good representation of the room temperature, T. In certain situations, however, it is not feasible to install a duct temperature sensor due to the fear that the electrical voltage supplied to the sensor may react with the volatile fumes. Under those situations, the room wall thermostat sensor can still be used and the room temperature can be estimated by a simple relationship between the room thermostat and using a temporary room air temperature sensor as below. The development of this model and its validation are discussed in detail by Ahmed (1996). The relation between the space temperature and the thermostat reading is

$$\frac{dT_{st}}{dt} = -C2_{st}(T_{st} - T).$$
(18)

The thermostat calibration constant, $C2_{st}$, can easily be found during the commissioning process by locating a temperature sensor in the exhaust duct temporarily or at a good location within the room; changing the room temperature set point; trending both thermostat temperature, T_{st}, and room air temperature, T, from a temporary location; and fitting the trended data to Equation 18 to determine $C2_{st}$. Once the thermostat constant is calibrated, the temperature sensor can be removed from the temporary location. As an alternative, the sensor to measure the room air temperature can be located in the general exhaust duct for the lab air only. The sensor in the general exhaust duct cannot be used continuously in lieu of the thermostat because, often, the general exhaust damper may be closed completely and the sensor will not be exposed to the room airflow. On the other hand, by having a sensor in the general exhaust, the calibration process can be automated to update the value of the calibration constant, $C2_{st}$, by using the trended sensor and the thermostat values in Equation 18.

RESULTS

Several cases are simulated and the results are discussed in the following sections.

CASE C1: Linear Damper with an Authority of 1.0

In cases C1, C2, and C3, a sudden increase in the internal heat generation rate is imposed as a disturbance. Referring to Figure 3, it should be noted that at time $t = 0$, there is a sudden disturbance in the load from 85.50 Btu/min (90 kJ/min) to 427.50 Btu/min (450 kJ/min) at time $t = 25$ minutes. Both PI and FFPI control loops are tuned for the linear damper/actuator characteristics. The supply and general exhaust characteristics are assumed to be the same for both controls. The tuning process was the same as explained earlier in discussing the pressure control sequence (Part I). The general exhaust damper flow loop was tuned first, followed by the supply flow loop. The tuning of the FFPI loop was relatively straightforward and simple with very small gains compared to the PI control loop, which was complex, time consuming, and had large gains. Once tuned, the loop parameters are kept unchanged for other cases. The gains are shown in Table 1.

Figure 6 illustrates the temperature response for both PI and FFPI control loops. Also included are the simulated and predicted loads to indicate that the predicted load agrees extremely well with the simulated load. The simulated load is calculated by adding the known internal load term and the calculated wall heat transfer. A good load prediction is a precondition of achieving good control.

Both the PI and FFPI performed well in terms of setpoint tracking accuracy and response time. While the PI control loop quickly settles to the desired set point of 70°F (21.11°C), the settling is gradual in the case of FFPI. However, the FF part

TABLE 1
Table of Controller Gains

Control Sequence	Control Equipment	FFPI Controller		PI Controller	
		P_g (Control Signal/Error)	$I_g S$ (Control Signal/Error)	P_g (Control Signal/Error)	$I_g S_t$ (Control Signal/Error)
Cooling	Supply Damper	3.0 e(-6)	2.5 e(-6)	0.00018	6.1e(-5)
	General Exhaust	3.0 e(-6)	2.5 e(-6)	0.3675	0.163
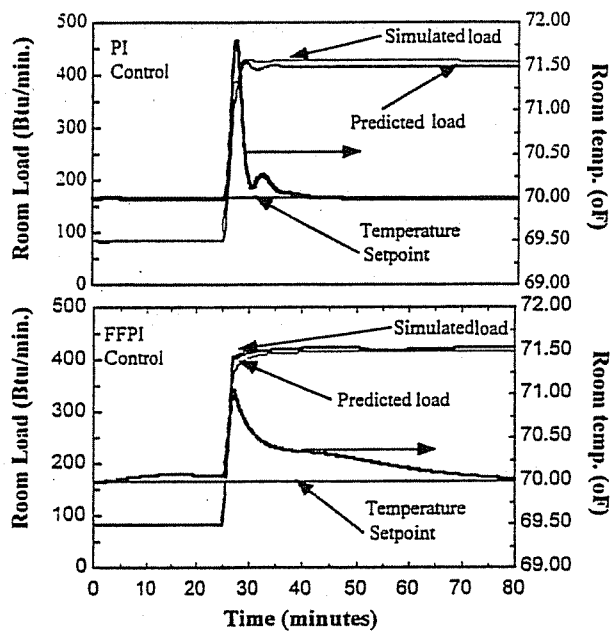
Figure 6   Dynamic response of room temperature and predicted load for control sequence C1.
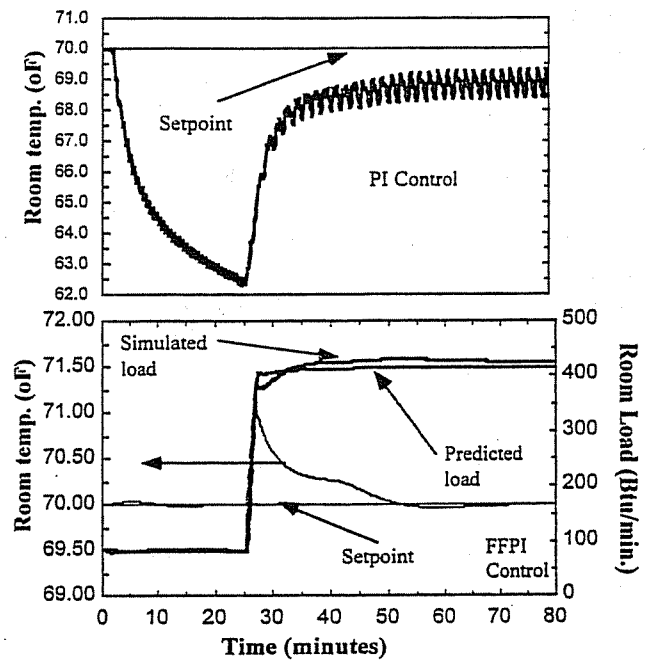
Figure 7   Dynamic response for room temperature and predicted load for control sequence C2.

of the loop brings the room temperature within 0.5°F (0.278°C) quickly, leaving only a small residual to be slowly handled by the PI component of the combination loop.

Case C2: Linear Damper with an Authority of 0.01

In this case, the nonlinear damper characteristics are assumed for both supply and general exhaust damper. As shown in Figure 7, the result for PI control shows poor performance as the room temperature continues to fall when the initial load is imposed, and then the room temperature oscillates due to a sudden increase in the load. As also shown in Figure 7, the FFPI control loop showed good control and held the temperature within a narrow range of 1°F (0.56°C). The predicted load matched the simulated load very well. For PI control, the predicted load is intentionally not shown as it has significant cycling. Instead, a plot of the cycling supply flow rate is of more practical value since such cycling contributes to noise and equipment failure, an often observed effect of poor HVAC control (Blazier 1993; Cerami 1996). Such plotting is included for the next case.

Case C3: Nonlinear Damper with W_f = 0.5 and an Authority of 0.5

As shown in Figure 8, in this case the PI control responds well to the initial load but shows poor control when the load is suddenly increased by fivefold. The FFPI control manages to control well throughout the simulation period. The supply flow rate plots for both control loops are shown in Figure 9, which indicates that the supply flow cycles between the maximum and minimum flows. These flow oscillations would be unacceptable and demonstrate the failure of the PI control loop. In contrast, the supply flow response for the FFPI loop is stable and tracks the desired set point well. Even with cycling of the supply flow loop, the temperature in the space oscillates in a narrow range of 1°F (0.56°C) (Figure 8). Although this small oscillation in space temperature might be hard to notice, the cycling will drastically shorten the life of the actuator.
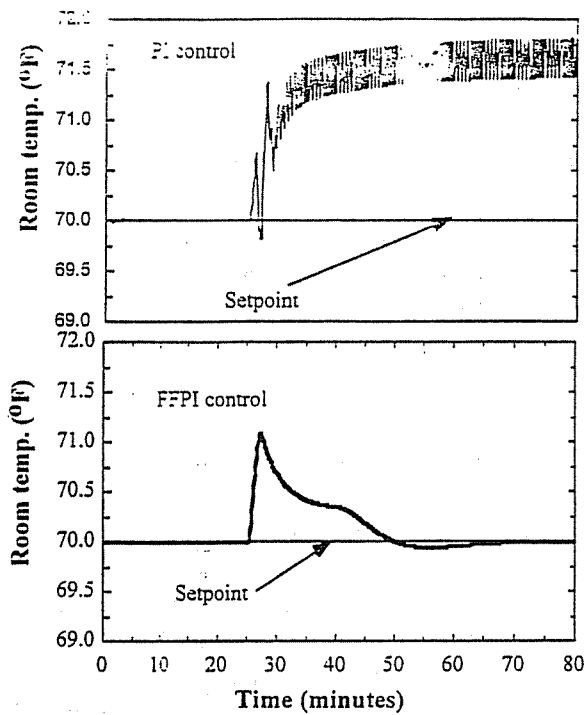
Figure 8 Dynamic response of room temperature response for control sequence C3.
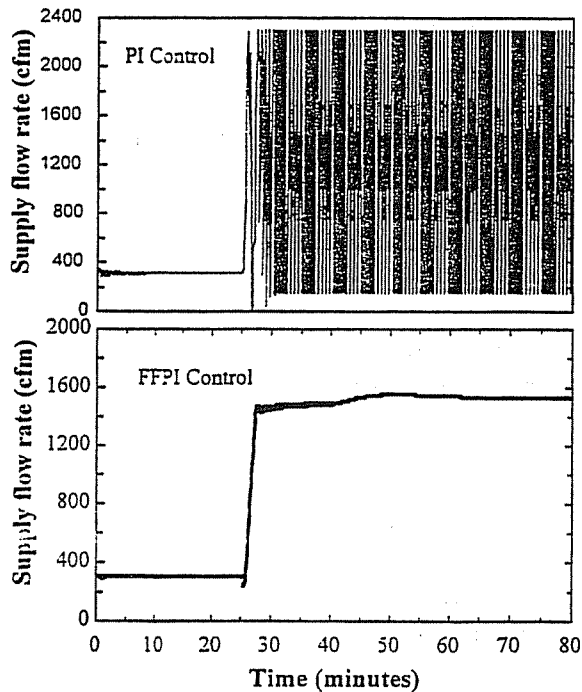

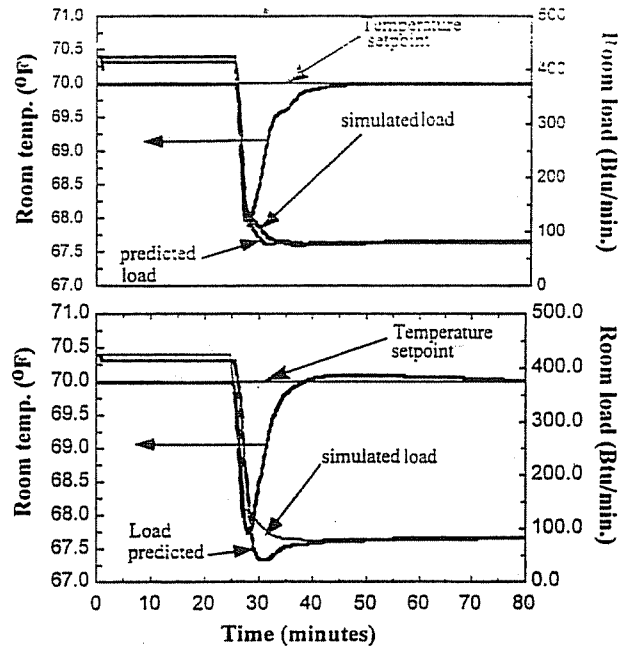Figure 9 Supply flow response for control sequence C3.

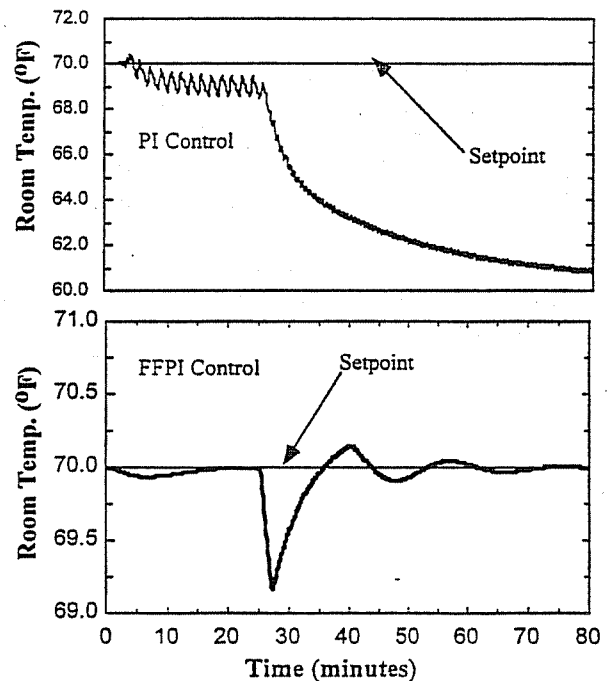Figure 10 Dynamic response of room temperature and predicted load for control sequence C4.

Figure 11 Dynamic response of room temperature control sequence C5.

Cases C4, C5, and C6: Temperature Control—Cooling for Decrease in Room Load

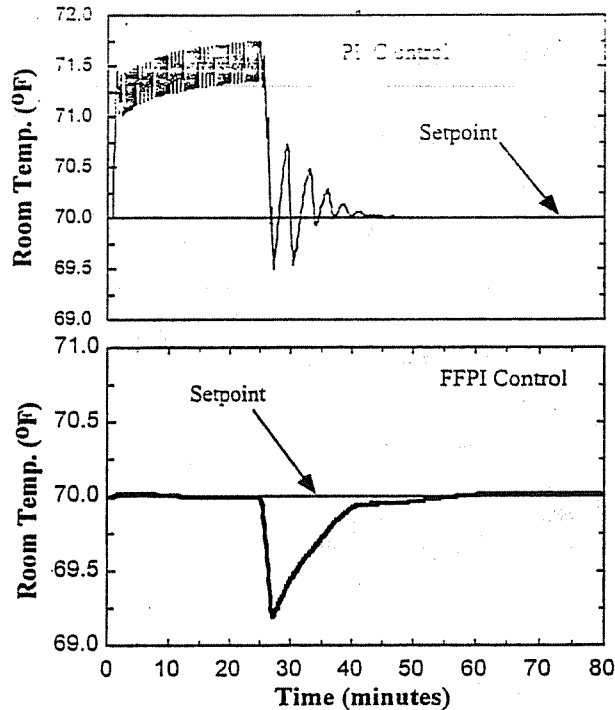In cases C4, C5, and C6 (Figures 10 through 12), internal load is suddenly decreased by fivefold from an initial steady

Figure 12 *Dynamic response of room temperature control sequence C6.*

value. These cases are just the opposite of cases C1, C2, and C3. The results are similar but are the reverse in the response when compared to cases C1, C2, and C3.

In case C4, for a linear damper with an authority of 1.0, both PI and FFPI control loops work very well. For a linear damper with an authority of 0.01 (case 2), the PI control performance deteriorates considerably. For the last case 6, for a nonlinear damper with an authority of 0.01, an instability again is observed at the high load and flow condition. However, when the load is decreased, the PI seems to provide good control. For all cases, the FFPI provides accurate and stable control.

SUMMARY

Cooling control is complicated due to the presence of dual coupled loops for the supply and general exhaust flows. The controllability of the general exhaust loop was very dependent on an accurate load prediction. The steady-state method of load prediction works well. It is feasible to implement the load prediction method in a real controller because it is simple. Since the load prediction method does not require any additional sensors or hardware, the proposed scheme may become cost-effective.

Similar to the pressure control sequence results, the FFPI control loop works well under a wide range of operating conditions, even subject to sudden extreme disturbances up to a fivefold increase in internal load generation. Compared to the PI control loop, the FFPI provides an excellent control.

NOMENCLATURE

c	=	specific heat, Btu/lbm·R (kJ/kg·K)
FF	=	feedforward
FFPI	=	combined feedforward and feedback
GRNN	=	general regression neural network
HVAC	=	heating, ventilating, and air conditioning
h	=	enthalpy, Btu/lbm (kJ/kg)
I_g	=	integral gain constant in PID controller
K_l	=	envelope leakage constant
Lab	=	laboratory
m	=	mass, lbm (kg)
$\dot{m}$	=	rate of mass flow, lbm/sec (kg/s)
n	=	flow exponent
P	=	pressure, inches of water (kPa)
ΔP	=	pressure differential, inches of water (kPa)
PI	=	proportional-integral
PID	=	proportional-integral-derivative
P_g	=	proportional gain constant in PID controller
$\dot{q}_{gen}$	=	the rate of generation of internal heat, Btu/min (W)
$\dot{q}_{load}$	=	room thermal load, Btu/min (W)
$\dot{q}_{tr}$	=	rate of heat transfer by conduction, Btu/min (W)
r	=	normalized actuator position (0-1)
r_a	=	command actuator position
R	=	gas constant, Btu/lbm·R (kJ/kg·K)
S_t	=	sample time, seconds
t	=	time
T	=	temperature, °F (°C)
U	=	total internal energy, Btu/lbm (kJ/kg)
V	=	volume, ft³ (m³)
VAV	=	variable air volume
$\dot{v}$	=	volumetric flow rate, ft³/min (m³/min)
W_f	=	nonlinear valve/damper parameter
w.c.	=	inches of water column gauge
w.g.	=	inches of water column gauge

Greek Symbols

ρ	=	density, lbm/ft³ (kg/m³)
τ	=	time constant, seconds

Subscripts

a	=	air
ad	=	adjacent space
e	=	exhaust
ex	=	general exhaust
fh	=	fume hood
gen	=	generation
i	=	in
o	=	out
p	=	constant pressure

s = supply

sp = set point

st = thermostat

$t - t_o$ = sample time equal to current sample time t preceded by dead time t_o

v = constant volume

REFERENCES

Ahmed, O. 1996. Model-based control of laboratory HVAC system. Ph.D. thesis, University of Wisconsin-Madison.

Ahmed, O., J.W. Mitchell., and S.A. Klein. 1998a. Feedforward-feedback controller using general regression neural network (GRNN) for laboratory HVAC system: Part I—Pressure control. *ASHRAE Transactions* 104(2).

Ahmed, O., J.W. Mitchell, and S.A. Klein. 1998b. Feedforward-feedback controller using general regression neural network (GRNN) for laboratory HVAC system: Part III—Temperature control—Heating. *ASHRAE Transactions* 104(2).

Blazier, W.E. 1993. Control of low frequency noise in HVAC air-handling equipment and systems. *ASHRAE Transactions* 99(2).

Cerami, V.J. 1996. Controlling HVAC equipment noise. *Heating/Piping/Air-Conditioning*.

Neuman, V.A. 1989. Design considerations for laboratory HVAC systems dynamics. *ASHRAE Transactions* 95(1).